sustainability

MDPI

Article

Analysis of Effects of Spatial Distributed Soil Properties and Soil Moisture Behavior on Hourly Streamflow Estimate through the Integration of SWAT and LSM

Seoro Lee [1], Kyoung Jae Lim [2] and Jonggun Kim [2,*]

[1] Agriculture and Life Sciences Research Institute, Kangwon National University, Chuncheon-si 24341, Republic of Korea; lopp3691@kangwon.ac.kr
[2] Department of Regional Infrastructure Engineering, Kangwon National University, Chuncheon-si 24341, Republic of Korea; kjlim@kangwon.ac.kr
* Correspondence: kimjg23@gmail.com

Abstract: This study addresses the challenge of accurately estimating hourly flow and soil moisture by integrating the Soil and Water Assessment Tool (SWAT) with a Land Surface Model (LSM). Our approach enhances SWAT by incorporating spatially distributed soil properties and a physically-based soil moisture process, using the Noah LSM for hourly soil moisture estimation. This integration captures spatial variations in soil moisture and hydraulic properties from remote sensing across the watershed. The parameter sensitivity analysis and the calibration of hourly flow were significantly impacted by the physically-based hourly soil moisture routing and the incorporation of spatially distributed soil properties. Consequently, the modified SWAT model showed improved accuracy in hourly flow simulations for long-term and multiple rainfall events. Validation results showed significant improvements, with Coefficient of Determination (R^2) and Nash and Sutcliffe Efficiency (NSE) increasing by 25.95% and 33.3%, respectively, and Percent Bias (PBIAS) decreasing by 85.8%. Notably, the average error for peak flows across eight events decreased by 49%. These findings highlight the importance of initializing soil parameters based on spatial soil moisture distribution and incorporating physical process-based moisture routing to enhance hourly flow simulation accuracy. Future research should focus on validating the physical feasibility of the soil parameter set in the study area with detailed hourly flow and soil moisture data and exploring its applicability in various regions. This study provides valuable insights for the scientific community, water resources, and agricultural decision-makers regarding integrated modeling of soil moisture and hourly flow, which can inform dam operation management, disaster planning, and crop yield improvement.

Keywords: SWAT; LSM; soil moisture dynamics; remote sensing; spatial distributed soil properties

check for updates

Citation: Lee, S.; Lim, K.J.; Kim, J. Analysis of Effects of Spatial Distributed Soil Properties and Soil Moisture Behavior on Hourly Streamflow Estimate through the Integration of SWAT and LSM. *Sustainability* **2024**, *16*, 1691. https://doi.org/10.3390/su16041691

Academic Editors: Lucio Di Matteo and Carla Ferreira

Received: 4 January 2024
Revised: 7 February 2024
Accepted: 16 February 2024
Published: 19 February 2024

1. Introduction

Flood disasters are a major concern in many regions of the world due to the recent increase in the frequency of short-duration floods caused by climate change [1–3]. In particular, short-duration rainfall extremes cause the collapse of irrigation structures and residential facilities, the burial of agricultural land, and the deterioration of river water quality, resulting in socioeconomic losses [4,5]. Therefore, timely and accurate sub-daily flow prediction is essential for understanding river dynamics through high-resolution temporal simulations, especially as climate change influences precipitation patterns. These predictions help policymakers prepare and develop appropriate watershed management strategies for flood risk mitigation.

Hydrological models, such as the Soil and Water Assessment Tool (SWAT) [6] and the Hydrologic Simulation Program-Fortran (HSPF) [7], are important tools that can be used in sub-daily flow prediction. Among them, the SWAT is a globally recognized hydrological modeling tool extensively utilized to efficiently evaluate hydrology and water resources in large-scale watersheds across various hydrologic and environmental simulations [8–11]. The sub-daily SWAT model developed by Jeong et al. [12] has demonstrated reasonable hourly flow simulation capabilities for both long-continuous periods and short-term events. Additionally, the performance of the sub-daily SWAT model has been successfully demonstrated in watersheds of various sizes [13,14]. However, the SWAT model simulates soil moisture using a simplified storage routing method based on daily processes, which may have challenges in accurately representing the physical behavior of soil moisture in both saturated and unsaturated soils. Qi et al. [15] developed the Richards-equation-based SWAT (RSWAT) model and evaluated the soil moisture prediction using data from 10 observation stations. Their results showed that the RSWAT model improved the surface soil moisture prediction compared to the original bucket soil moisture algorithm within the SWAT model. This emphasizes that the physical process-based soil moisture algorithm in the hydrological model contributed to better capturing the dynamic characteristics of soil–water interactions. In addition, in the SWAT model, the same hydrological soil properties values are assigned to hydrological response units according to the given soil type due to its semi-distributed structure [16]. Shin et al. [17] found that employing a hydrological connectivity index, which is based on physical properties, can effectively explain the spatial variation in soil moisture and enhance the performance of the SWAT model when using spatially distributed soil hydraulic parameters. The soil moisture has high temporal and spatial variability in watersheds and can significantly impact flow patterns and magnitudes [18–20]. A realistic modeling approach is essential for reliable hourly flow simulation, capturing the spatial distribution of soil properties and moisture behavior. However, accurately reflecting these elements is a complex and challenging task in the domain of hydrological modeling.

The Noah Land Surface Model (Noah LSM) is a model based on energy equations and water balance equations that can be combined with various models to improve hydrologic simulation performance [21–24]. The Noah LSM is capable of simulating soil moisture in saturated and unsaturated zones based on the Richards equation [25]. In addition, recently, an assimilation method using soil moisture image data observed by remote sensing has been applied to improve the ability of the model by reducing uncertainty about the hydrology and soil parameters. According to previous sub-hourly SWAT modeling studies, due to limitations in collecting hourly observation data, it is common to evaluate model performance through calibration and validation using hourly flow data observed in the watershed. Even if model performance calibrated using only streamflow data without adequate consideration of the spatial patterns of hydrologic phenomena within the watershed may be statistically significant, it may lead to inaccurate results for ungauged areas [26]. This may cause difficulties in interpreting the flow simulation results from the perspective of the watershed water cycle or accurately assessing the effect on best management practices. Nevertheless, few studies have proposed approaches to spatially distribute physical soil properties within watersheds for potential agreement with remote sensing soil moisture in hourly simulations with the SWAT model.

In the present study, we integrate the Richards-equation-based soil moisture module of the Noah LSM with the SWAT model to simulate hourly flow and soil moisture. Subsequently, we redistributed the properties of soil parameters (here, saturated hydraulic conductivity, available water capacity, and bulk density) of the SWAT model using remotely sensed soil moisture data. Especially, the main objective of this study is to investigate the impacts of physical soil moisture behavior and the spatial soil characteristics on hourly flow simulations. This study highlights that the integration of models such as the SWAT and Noah LSM models is important for improving our understanding of the interaction between soil moisture and streamflow and achieving accurate hydrological simulations at the watershed scale.

2. Materials and Methods

2.1. Description of the Study Area

The study area is located in the Seokwon watershed in South Korea (Figure 1). The watershed covers an area of 52 km^2 with a mainstream length of approximately 15.8 km. The watershed has an average elevation of 118.4 m and a slope of 14.1%. The land use was classified into eight categories: urban (7.8%), rice field (25.6%), field (21.6%), orchard (1.6%), forest (29.8%), pasture (0.6%), bermudagrass (10.2%), and water (2.8%). The soil in the watershed is composed of six distinct soil types, characterized by their respective soil codes and compositions: Sandy Loam represented by Ma (12.4%), Re (17.2%), and Ra (41.2%); Silty Clay Loam represented by Ap (10.5%) and An (16.2%); Loamy Sand represented by Af (2.5%). The spatial distribution of land use types, soil codes, and slope is shown in Figure 2. In this study area, the average annual precipitation and temperature for the last few years (2017–2021) were 1137 mm (772–1688 mm) and 12.46 °C (11.74–12.77 °C), respectively.

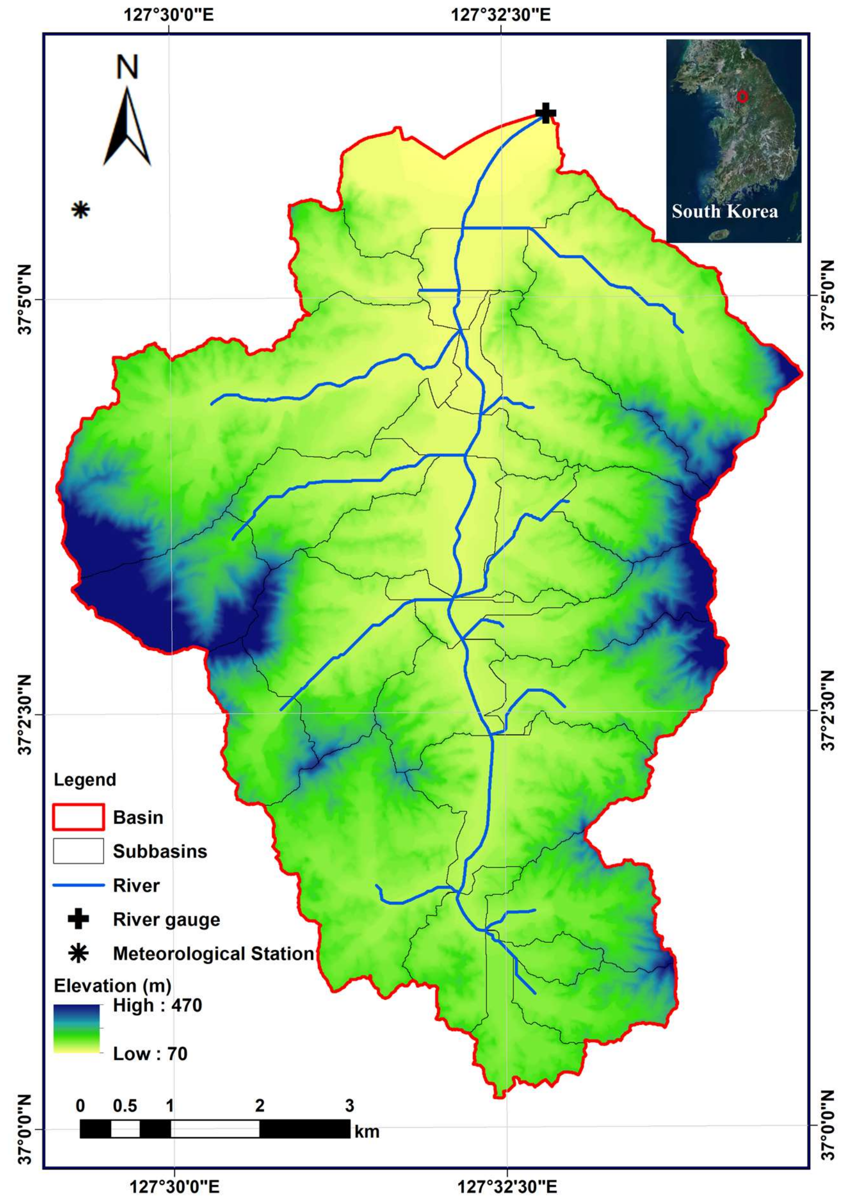

Figure 1. Location of the study area.

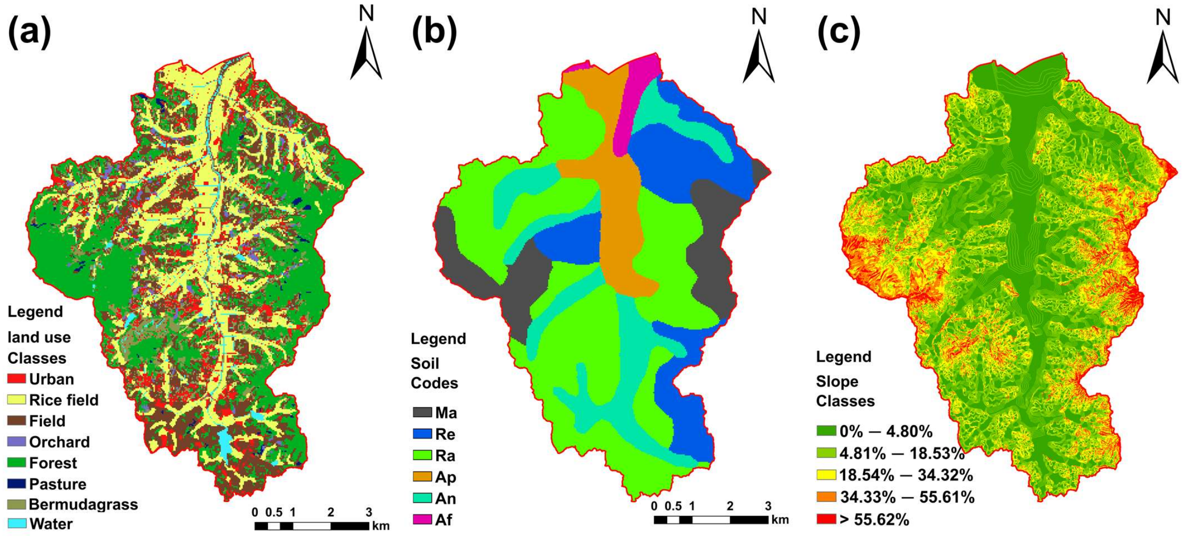

Figure 2. Major characteristics in the study area. (**a**) Land use types, (**b**) soil codes, and (**c**) slope.

2.2. SWAT Model

The SWAT model is a semi-distributed watershed model developed by the United States Department of Agriculture Agricultural Research Service [6]. It divides a watershed into subbasins and subdivides them into Hydrologic Response Units (HRUs) based on the combination of land use, soil, and slope within the subbasins. The hydrologic cycle of each HRU is simulated based on the water balance, including rainfall, surface runoff, evaporation, and percolation. The simulated flow from the HRU is summed for each subbasin and flows into the mainstream of the corresponding subbasin, and is routed by the variable storage routing method [27] and Muskingum routing method [28]. Detailed descriptions and calculation formulas for each hydrologic component are provided in the SWAT theoretical documentation [29].

In the SWAT model, infiltration is calculated through the Green–Ampt Mein–Larson (GAML) [30] excess rainfall method, which uses a simple storage routing method based on daily processes to determine hourly surface flow. The GAML method assumes that the soil profile is homogeneous and that the antecedent moisture is uniformly distributed within the soil profile [12]. The GAML infiltration rate is expressed through Equation (1) [29].

$$f(t) = K_e \times \left(1 + \frac{\Psi \times \Delta\theta}{F(t)}\right) \tag{1}$$

where $f(t)$ is the infiltration rate at time t, (mm/h), K_e is the effective hydraulic conductivity (mm/h) considering the effects of saturated hydraulic conductivity and curve number [31], Ψ is the wetting front matric potential (mm), $\Delta\theta$ is the change in volumetric soil moisture content across the wetting front (mm/mm), and $F(t)$ is the cumulative infiltration rate at time t (mm).

2.3. Noah Land Surface Model (LSM)

In this study, we used the Noah LSM [32] of the National Centers for Environmental Prediction to link with the SWAT model. The Noah LSM sets the initial thickness of the soil to 2 m, with layer boundaries at 0.1, 0.4, 1.0, and 2.0 m. Soil moisture in each soil layer is simulated through the diffusion form of the highly nonlinear Richards equation [33] (Equation (2)), which is derived from Darcy's law and the continuity equation [34]. This means that the soil moisture in the soil layer always percolates into the deeper soil layer by convective flow, and soil moisture gradients cause the upward or downward movement of water [35]. The matric potential and hydraulic conductivity of unsaturated soils are described by the equations of Clapp and Hornberger [36] (Equations (3) and (4)), respectively.

$$\frac{\partial\theta}{\partial t} = \frac{\partial}{\partial z}\left(D\frac{\partial\theta}{\partial z}\right) + \frac{\partial K(\theta)}{\partial z} + S(\theta) \tag{2}$$

$$\Psi(\theta) = \Psi_{sat}\left(\frac{\theta}{\theta_{sat}}\right)^{-b} \tag{3}$$

$$K(\theta) = K_{sat}\left(\frac{\theta}{\theta_{sat}}\right)^{2b+3} \tag{4}$$

where θ is the soil moisture content (m^3/m^3), D is the soil water diffusivity (m^2/s), $K(\theta)$ is the hydraulic conductivity (m s^{-1}), S represents the sources and sinks (i.e., transpiration, evaporation, and rainfall) (m/s), t and z represent the time and the vertical height (s and m, respectively), $\Psi(\theta)$ is the metric potential of unsaturated soil, Ψ_{sat} is the metric potential of saturated soil (m/s), θ_{sat} is the saturated soil moisture content (m^3/m^3), K_{sat} is the saturated hydraulic conductivity (m/s), and b represents the curve fitting parameter (unitless) related to the pore size distribution.

2.4. Integrating the SWAT and Noah LSM

In this study, we linked the SWAT model and Noah LSM to simulate hourly flow in the watershed, reflecting soil moisture behavior in saturated and unsaturated conditions according to the hourly rainfall. The modified SWAT model uses the GAML and Richards equation to simulate the soil moisture content, infiltration, and surface flow in the soil layer at hourly time steps for each HRU in the watershed (Figure 3). Surface characteristics such as soil type, land use, and slope for each HRU are internally used in the soil process of Noah LSM to determine the main soil parameters including BB (Function of Soil Type), SATPSI (Saturation Soil Potential), and QTZ (Soil Quartz Content). The values of each soil parameter according to the soil type were used as the default values presented in Niu et al. [37].

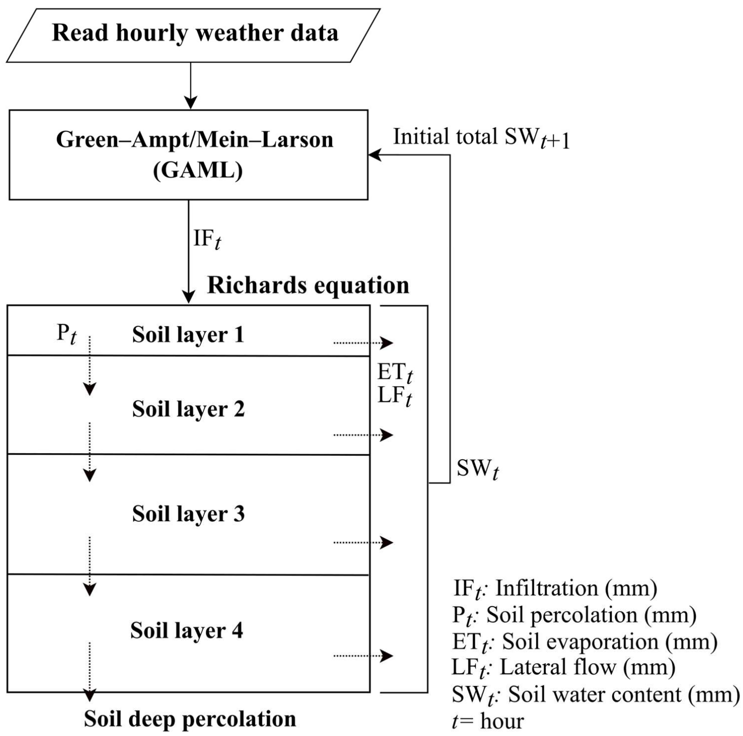

Figure 3. Schematic of soil moisture simulation through Richards equation and GAML linkage.

The initial infiltration value for each HRU, calculated using GAML, was used to simulate soil moisture behavior in each soil layer of the Noah LSM. Subsequently, in the Noah LSM, hourly hydrological processes, such as soil moisture, lateral flow, percolation, and evaporation, were then performed in each soil layer. The soil moisture value for the entire soil layer simulated through the Noah LSM was updated with the initial soil moisture value at the next time ($t + 1$) in GAML and used to simulate infiltration and surface flow. The amount of hourly lateral flow and percolation in the last layer simulated through the Noah LSM was converted into the daily units and transmitted to the SWAT model and used for channel routing.

2.5. Spatial Distribution of Soil Parameters Based on Remotely Sensed Soil Moisture Data

The Sentinel-1 A/B satellite of the European Space Agency (ESA) provides high-resolution (10 × 10 m) Synthetic Aperture Radar (SAR) data and orbits with a revisit cycle of 12 d. The SAR backscattering coefficient, which is the magnitude of the microwave signal received from the surface, is closely related to the soil moisture content [38]. Therefore, the characteristics of the backscattering coefficient have been utilized for flood mapping in various areas for natural risk management and land use planning [39,40]. Additionally, studies have been conducted for soil moisture mapping at the regional and field scales through linear regression analysis between the backscattering coefficient and the soil moisture observed at the surface [41–44].

In this study, to derive a spatial distribution map of soil moisture in the Seokwon watershed, image data observed from the Sentinel-1 satellite from June to October 2018 were preprocessed to construct the backscatter coefficient data. Due to the limited availability of observed soil moisture data in this study area, a linear regression equation was derived from the backscattering coefficient of the region located near the watershed and the soil moisture observation data for 18 points. The regression equation was used to calculate the soil moisture value for each HRU.

To ensure the potential agreement of soil moisture, the initial values of the main hydrological soil parameters (SOL_K, SOL_AWC, and SOL_BD) were redistributed based on the five sections separated by the quartile reference values of the box plot for the soil moisture values. The properties of the spatially distributed soil parameters were updated with the necessary parameters for simulating soil moisture behavior in the Noah LSM during the process of linking the two models. Within the Noah LSM, the SATDK (Saturated Soil Conductivity) of the soil was replaced with the average value of SOL_K for the soil layers, and the MAXSMC (Max Soil Moisture Porosity) was replaced with a value calculated using SOL_BD. Figure 4 shows a schematic diagram of the spatial distribution method for properties of hydrological soil parameters using remotely sensed soil moisture data.

2.6. Model Inputs and Setup

To simulate the SWAT model, several types of data are required, including a Digital Elevation Model (DEM), a land use map, a soil map, and meteorological data. In this study, we used 5 × 5 m resolution DEM data that was constructed using 1:5000 digital topographic maps for watershed delineation. For the land use and soil maps, we used medium-class land use maps at a scale of 1:25,000 and soil maps at a scale of 1:50,000, respectively.

The watershed was divided into 27 subbasins using the DEM data, and a total of 1079 HRUs were generated based on surface characteristics, such as soil, land cover, and slope. Hourly meteorological data (rainfall, temperature, relative humidity, atmospheric pressure, insolation, and wind speed) for the simulation period (January 2020–July 2022) were collected from the Iljuk station located near the watershed. The hourly SWAT model simulation was performed for three years (2020–2022), including a one-year warm-up period in 2020.

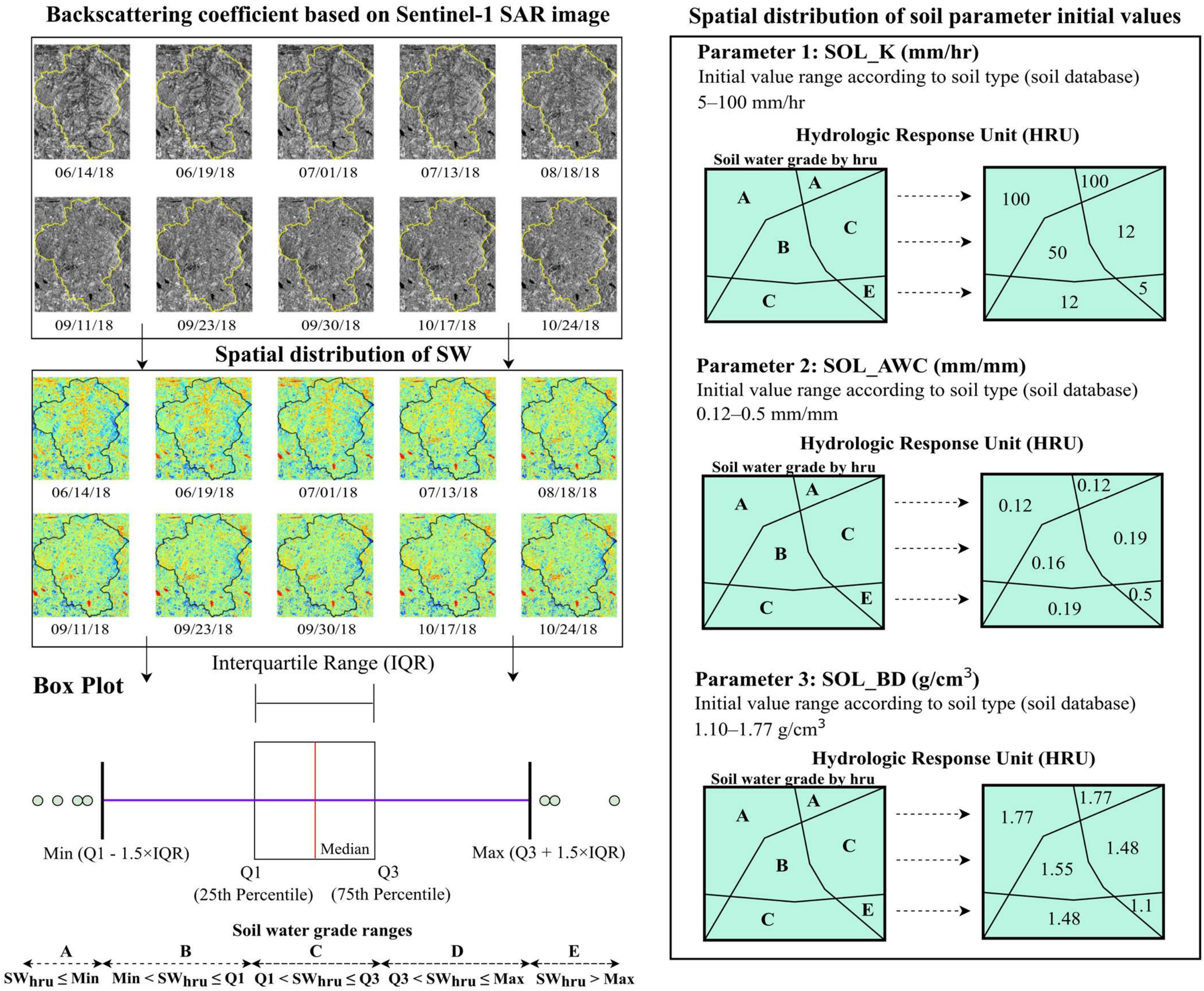

Figure 4. Spatial distribution method for properties of hydrological soil parameters using remotely sensed soil moisture data.

Table 1 summarizes the sources and input data used in the model.

Table 1. SWAT model input data and sources.

Data Type	Resolution	Source	Description
DEM	5 × 5 m	National Geographic Information Institute https://www.ngii.go.kr, accessed on 8 February 2024.	Digital elevation model
Land use	30 × 30 m (1:25,000)	Environmental Geographic Information Service https://egis.me.go.kr, accessed on 8 February 2024.	Land use map
Soil	30 × 30 m (1:50,000)	Rural Development Administration http://soil.rda.go.kr, accessed on 8 February 2024.	Soil map
Weather data	1 gauge	Korea Meteorological Administration https://www.weather.go.kr, accessed on 8 February 2024.	Sub-daily weather data for 2020–2022

2.7. Model Calibration, Validation, and Sensitivity Analysis

The SWAT model simulates hydrological processes using many different parameters, and therefore, calibration to reduce parameter uncertainty is essential [45]. Many studies have used the SWAT-Calibration and Uncertainty Programs (SWAT-CUPs) [46] to automatically calibrate the parameters of the SWAT model and interpret its uncertainty [14,47–51]. The algorithm selected in SWAT-CUP optimizes the parameters to minimize the objective function [52]. In particular, the sequential uncertainty fitting algorithm v.2 (SUFI-2) of SWAT-CUP has been reported to quantify the uncertainty of parameters using the multivariate uniform distribution of the hypercube and generate a reasonable and balanced prediction result [53]. Recently, the SWAT-CUP user group (swat-cup@googlegroup.com) shared an additional package of SWAT-CUP for hourly SWAT model calibration and validation.

This study performed calibration (from 9 April 2021 to 21 October 2021) and validation (from 1 March 2022 to 26 July 2022) of the original and modified SWAT model's hourly flow using SUFI-2 of SWAT-CUP. The number of simulations run by SWAT-CUP for calibration was set to 1000 for both models. The calibration parameters of the SWAT model presented in Table 2 were selected from other related studies [12,14,54]. After the calibration process, a global sensitivity analysis was performed on the calibration parameters in terms of *t*-test and *p*-value. The sensitivity of the parameter is larger when the absolute value of the *t*-test value is larger and the *p*-value is smaller [55]. The goodness-of-fit of the simulated and observed values of the two models was evaluated using statistical metrics, such as the Coefficient of Determination (R^2) [56], Nash and Sutcliffe Efficiency (NSE) [57], and Percent Bias (PBIAS) [58]. The R^2 value is an indicator of the strength between the observed and simulated values, ranging from zero to one. The NSE value is a normalized statistic that determines the relative magnitude of the model variance compared to the observed data variance. The NSE value ranges from $-\infty$ to one; if the value is one, it means that the simulated value and the observed value are same. The PBIAS indicates whether the simulated value is greater or less than the observed data. If the PBIAS is positive, the model is underestimated, and if it is negative, it is overestimated. The flow prediction performance of the watershed scale model is evaluated as "satisfactory" if $R^2 > 0.60$, NSE > 0.50, and PBIAS $\leq \pm 15\%$ [59].

Table 2. Calibrated parameters of SWAT model. "R" indicates that the default parameter is multiplied by (1 + a given value) and "V" indicates that the default parameter will be replaced by a given value.

Parameter *	Definition of Parameter	Model Processes (File Name)	Type of Change	Initial Range	
				Min.	Max.
ALPHA_BF	Base flow recession constant (d)	Groundwater (.gw)	V	0.001	1
RCHRG_DP	Deep aquifer percolation fraction	Groundwater (.gw)	V	0.35	0.75
GW_DELAY	Delay time for aquifer recharge (d)	Groundwater (.gw)	V	0	100
GWQMN	Threshold water level in the shallow aquifer for base flow (mm)	Groundwater (.gw)	V	0.01	300
CH_K1	Effective hydraulic conductivity for tributaries (mm/h)	Subbasin (.sub)	V	0.025	150
CH_N1	Manning's n value for tributaries	Subbasin (.sub)	V	0.01	0.07
CH_K2	Effective hydraulic conductivity for the main channel (mm/h)	Channel route (.rte)	V	0.025	150
CH_N2	Manning's n value for the main channel	Channel route (.rte)	V	0.01	0.07
ALPHA_BNK	Baseflow alpha factor for bank storage (d)	Channel route (.rte)	V	0	1
HRU_SLP	Average slope steepness	HRU (.hru)	R	–0.2	0.2
LAT_TTIME	Lateral flow travel time (d)	HRU (.hru)	V	0	100
MSK_CO1	Weighting factor for influence of normal flow on storage time constant value	Basin (.bsn)	V	0.01	1
MSK_CO2	Weighting factor for influence of low flow on storage time constant value	Basin (.bsn)	V	0.01	1
SOL_K	Saturated hydraulic conductivity (mm/h)	Soil (.sol)	R	–0.5	0.5
SOL_AWC	Available water capacity of the soil layer (mm H_2O/mm soil)	Soil (.sol)	R	–0.25	0.25
SOL_BD	Moist bulk density (g/cm^3)	Soil (.sol)	R	–0.30	0.30
CN2	Soil Conservation Service (SCS) runoff curve number for moisture condition II	HRU management (.mgt)	R	–0.20	0.20

* Parameters for SWAT are defined in accordance with the guidelines provided in the SWAT User Manual [60].

3. Results

3.1. Sensitivity Analysis Results

Table 3 presents the optimal values and sensitivity rankings of parameters used for hourly flow calibration and validation of original and modified SWAT models. The sensitivity ranking was determined by the *t*-test and *p*-value, with parameters having *p*-values less than 0.03 considered sensitive.

Table 3. Calibrated parameters of original and modified SWAT models.

Parameter	Original SWAT			Modified SWAT		
	t-Stat	*p*-Value	Calibrated Value	t-Stat	*p*-Value	Calibrated Value
CN2	36.14	0.00	0.19	25.87	0.00	−0.16
CH_N2	−15.45	0.00	0.022	−21.88	0.00	0.013
CH_K2	−14.43	0.00	13.65	−13.59	0.00	22.14
LAT_TTIME	−6.76	0.00	0.44	−11.68	0.00	51.63
MSK_CO2	−4.90	0.00	0.54	−7.9	0.00	1.32
SOL_K	−3.94	0.00	−0.26	−3.04	0.00	−0.038
GW_DELAY	−3.77	0.00	44.49	0.87	0.39	32.13
ALPHA_BNK	3.55	0.00	0.72	5.71	0.00	0.75
RCHRG_DP	−3.21	0.00	0.42	−0.17	0.87	0.62
SOL_BD	−3.03	0.00	−0.05	−2.29	0.02	0.078
HRU_SLP	2.18	0.03	−0.023	−1.96	0.05	0.012
SOL_AWC	−2.02	0.04	0.20	−4.06	0.00	−0.13
CH_N1	−1.23	0.22	0.02	−0.44	0.66	0.05
CH_K1	−0.94	0.35	7.97	−1.29	0.19	69.13
ALPHA_BF	0.77	0.44	0.50	−0.59	0.55	0.43
MSK_CO1	0.57	0.57	0.91	−0.85	0.40	0.85
GWQMN	0.23	0.82	173.42	0.36	0.72	233.63

The initial Soil Conservation Service (SCS) runoff curve number for moisture condition II (CN2), Manning's "*n*" value of the main channel (CH_N2), effective hydraulic conductivity in main channel alluvium (CH_K2), lateral flow travel time (LAT_TTIME), coefficient of minimum flow storage time constant (MSK_CO2), saturated hydraulic conductivity (SOL_K), baseflow alpha factor for bank storage (ALPHA_BNK), and moist soil bulk density (SOL_BD) were determined as common sensitive parameters in both models. In particular, the three most sensitive parameters in both models were in the order of CH2, CH_N2, and CH_K2.

CN2 is directly used to calculate the effective hydraulic conductivity of GAML, with higher values leading to increased peak flow. The calibrated CN2 value, which controls surface runoff and is related to the land coverage characteristics, was increased by 19% for the original SWAT model and reduced by 16% for the modified model. Given that the terrain is the same for both models, an increased CN2 would increase surface runoff for the original model and reduce it in the modified version. This would imply that less water is available for infiltration in the original model in comparison to the modified model.

CH_N2 is the roughness of the river bed, and a high value induces a decrease in the velocity and rate of the flow. In the original model, the calibrated CH_N2 value (0.022) is representative of natural streams. However, in the modified model, the CH_N2 value (0.013) is representative of concrete channels. This suggests that sophisticated modeling is needed to accurately reflect current river characteristics, including improved artificial channels and various hydrological conditions, as well as natural river characteristics.

Higher values of CH_K2 induce water loss from the stream bed to the groundwater along the soil layer [61]. In the modified model, the calibrated value of CH_K2 was 22.14 (mm/h), causing greater groundwater loss within the river bed than in the original SWAT model.

3.2. Spatiotemporal Analysis of Soil Moisture Simulation Results

Figure 5 illustrates the temporal changes in soil moisture for each soil layer of a specific HRU, as simulated by the calibrated original and modified SWAT models. The hourly soil moisture of the original SWAT model indicates that the daily soil moisture remains constant for 24 h. However, the modified SWAT model simulated soil moisture by soil layer, on average, 14% higher than that of the original SWAT model. This is because the antecedent moisture content calculated during the model warm-up period was different due to the difference between the initial values of the soil parameters used in the two models and the soil moisture algorithm. In the modified SWAT model, soil moisture variations in the deep soil layer were greater than in the original SWAT model. This appears to be the effect of continuously simulating percolation amount in the vertical downward direction even in unsaturated soil in the modified SWAT model.

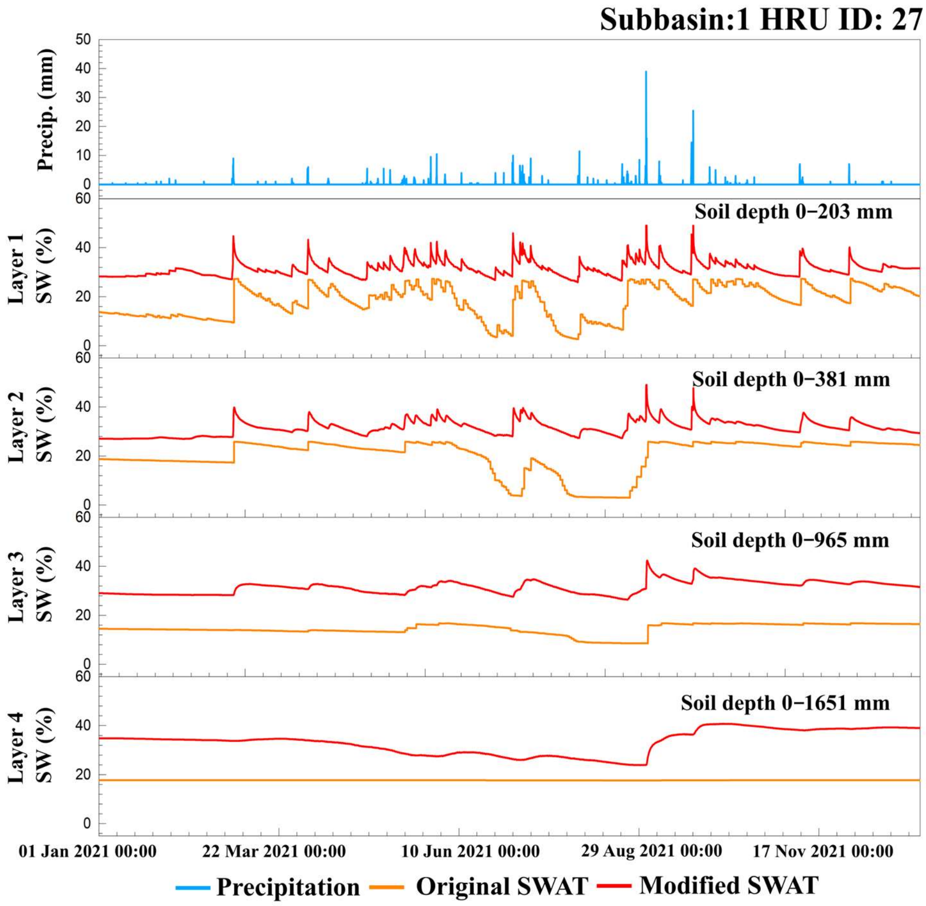

Figure 5. Temporal soil moisture variation pattern by soil layer.

Specifically, as shown in Figure 6, the original SWAT model simulates the soil moisture according to the daily rainfall, without considering the rainfall occurrence time. In contrast, the modified SWAT model causes a change in soil moisture based on the hourly rainfall. This means that the modified SWAT model can consider the effect of temporally changing soil matric potential when simulating hourly flow.

Figure 7 compares the spatial distribution of soil water content (%) within a watershed as obtained from remote sensing with the estimates from two SWAT models on 31 August 2021. The soil moisture content simulated by the original SWAT model showed a concentration of moisture content in the range of 21% to 30% in areas adjacent to the river, with lower moisture content below 20% distributed in other areas (Figure 7b). Particularly, the content of soil moisture was determined by the boundaries of the soil map, suggesting that soil properties dependent on soil map data play a significant role in the estimation of soil moisture. In contrast, as shown in Figure 7c, the soil moisture content simulated by the modified SWAT model showed a broad range of moisture content distributed across the watershed regardless of the soil map boundaries, similar to the remotely sensed soil moisture content data (Figure 7a).

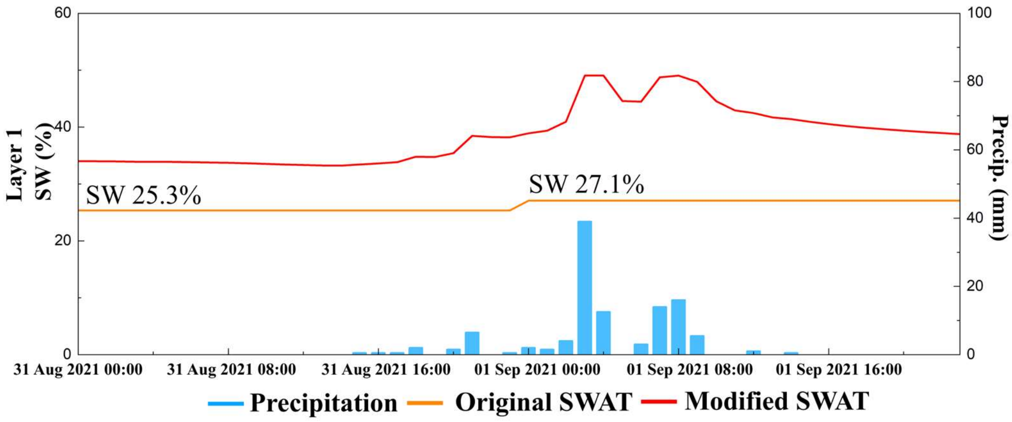

Figure 6. Soil moisture simulation results in the first layer of a specific HRU.

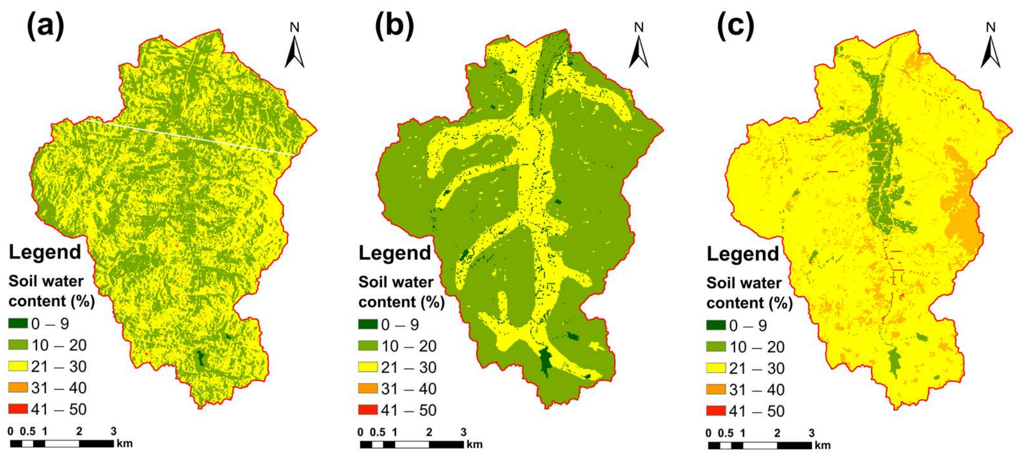

Figure 7. Spatial distribution of soil moisture in the watershed: (**a**) using remote sensing data, (**b**) with the original SWAT model, and (**c**) with the modified SWAT model.

3.3. Comparison of Model Performance for Calibration and Validation

Figure 8 shows the long-term hourly flow simulation results of the original and modified SWAT models during the calibration and validation period. The original SWAT model had an R^2 of 0.75 and 0.58, NSE of 0.62 and 0.54, and PBIAS of 71.4% and 65.5% during calibration and validation, respectively (Figure 8a). Although the performance of the original SWAT model for calibration was evaluated as "satisfactory" in terms of R^2 and NSE, its PBIAS showed poor performance in both calibration and validation periods due to its inability to capture low flows during non-rainfall [62,63]. By contrast, the modified SWAT model had an R^2 of 0.76 and 0.73, NSE of 0.75 and 0.72, and PBIAS of 18.8% and 9.3% during calibration and validation, respectively, resulting in a better "satisfactory" performance (Figure 8b). The modified SWAT model showed improved hourly flow prediction performance compared to the original model, with satisfactory values for R^2, NSE, and PBIAS. Notably, the validation performance of the modified SWAT model showed significant improvements over the original model, with R^2 and NSE increasing by 25.95% and 33.3%, respectively and PBIAS decreasing by 85.8%.

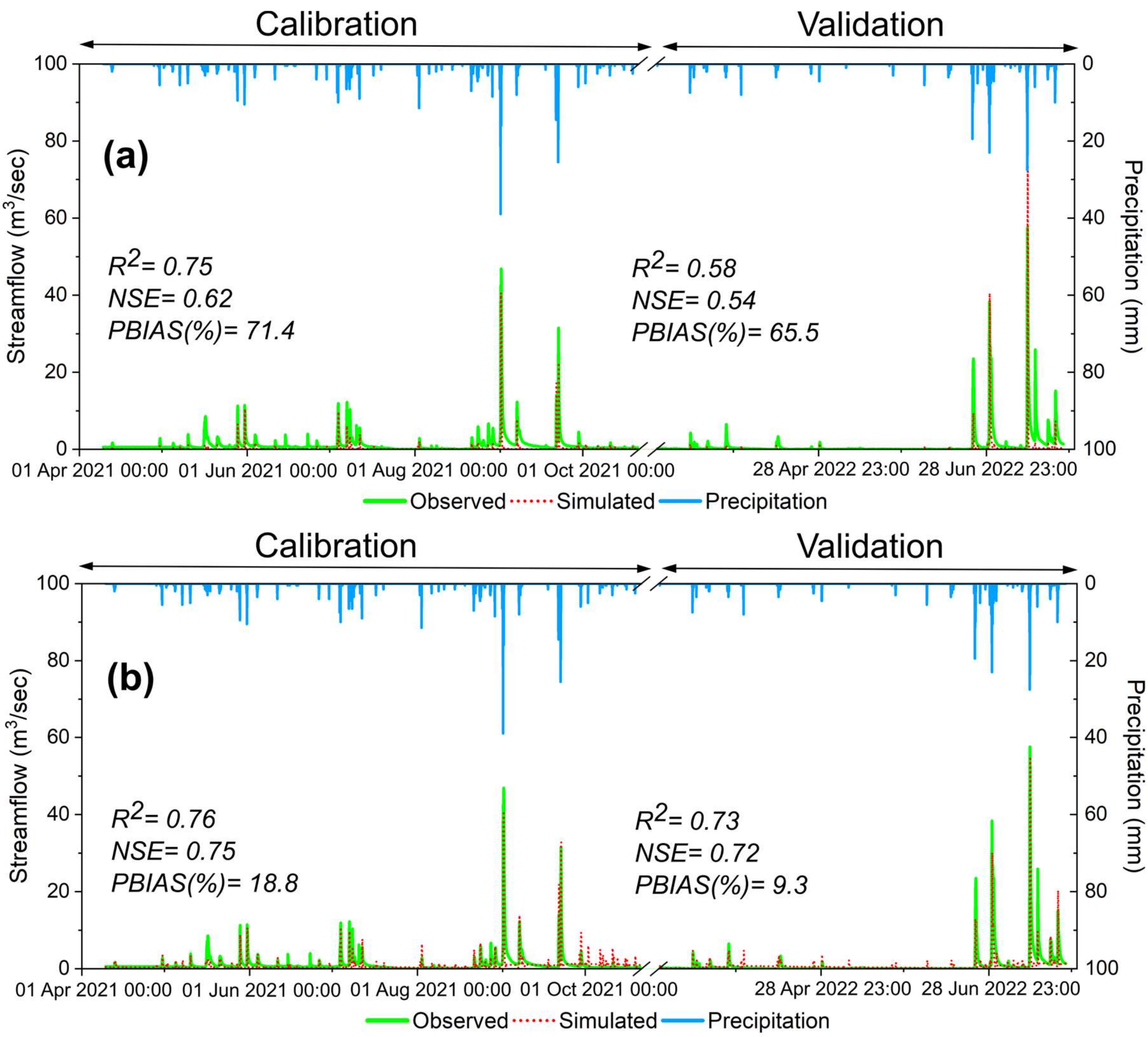

Figure 8. Hourly flow calibration and validation results of the (**a**) original SWAT model and (**b**) modified SWAT model.

3.4. Results of Hourly Flow Comparison by Rainfall Events

Figure 9 shows the hourly hydrologic graph that compares the observed and simulated values of the two models for eight rainfall events. The statistical performance results of both models for each rainfall event are summarized in Table 4. The average predictive performance of the modified SWAT model for rainfall events (R^2 = 0.79, NSE = 0.64, and PBIAS = 29.6%) was superior to that of the original SWAT model (R^2 = 0.66, NSE = 0.25, and PBIAS = 53%). In particular, the average percent error for peak flows across eight rainfall events also decreased by 49%. This is because of the influence of the soil moisture content, which changes according to the hourly rainfall, on the modified SWAT model's calibration for the antecedent soil moisture conditions in the watershed.

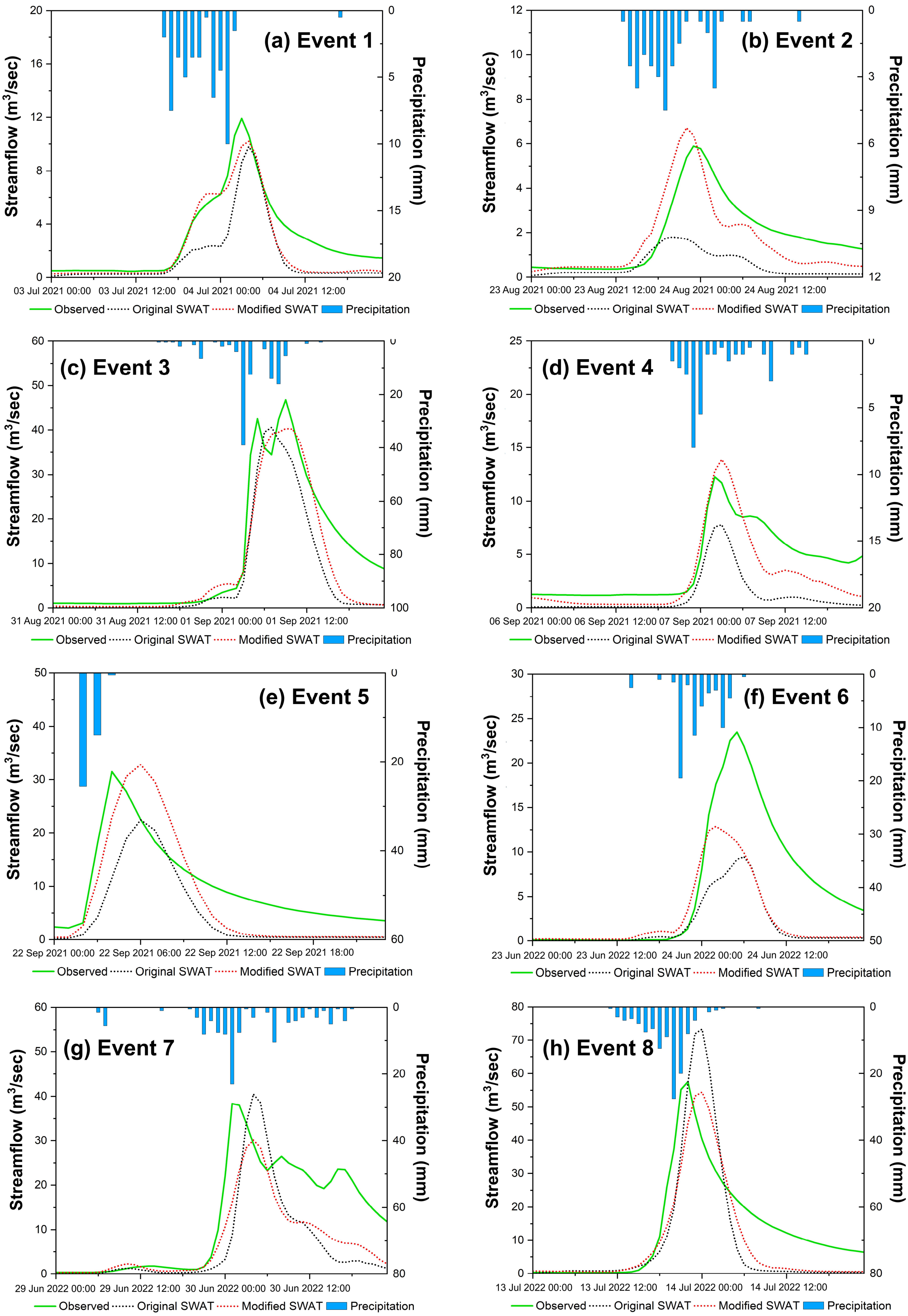

Figure 9. Observed and simulated streamflow for the calibration and validation events.

Table 4. Statistical performance results of original SWAT and modified SWAT models for rainfall events.

Event ID	Start Date	Rainfall (mm)	Observed Peak Flow (m^3/s)	Original SWAT					Modified SWAT				
				Peak Flow					Peak Flow				
				Simulated (m^3/s)	Percent Error (%)	R^2	NSE	PBIAS (%)	Simulated (m^3/s)	Percent Error (%)	R^2	NSE	PBIAS (%)
1	03 Jul 2021	49	11.9	9.80	17.6	0.82	0.60	47.4	10.2	14.3	0.90	0.84	25.1
2	23 Aug 2021	30	5.89	1.80	69.4	0.52	−0.33	70.9	6.71	13.9	0.75	0.68	11.5
3	31 Aug 2021	111	46.8	40.6	13.2	0.85	0.75	38.5	40.3	13.9	0.88	0.84	23.9
4	06 Sep 2021	33	12.3	7.78	36.7	0.66	−0.18	71.9	13.9	13.0	0.81	0.64	28.1
5	22 Sep 2021	40	31.5	22.5	28.6	0.39	0.26	51.7	32.8	4.1	0.80	0.50	21.4
6	23 Jun 2022	65.5	23.5	9.44	59.8	0.81	0.22	70.4	12.9	45.1	0.66	0.39	55.3
7	29 Jun 2022	111	38.4	40.5	5.5	0.50	0.23	47.5	30.1	21.6	0.74	0.51	42.6
8	13 Jul 2022	114.5	57.6	73.4	27.4	0.70	0.43	25.5	54.5	5.4	0.77	0.69	28.6
Ave.		69.3	28.5	25.7	32.3	0.66	0.25	53	25.2	16.4	0.79	0.64	29.6

Major rainfall events caused by excessive rainfall were analyzed using both models. For event 3 (precipitation 111 mm, peak flow 46.8 m^3/s), the modified model better predicted the peak flow (40.3 m^3/s) at the observation time (01 September 2021 09:00 h), while the original model simulated it 2 h earlier (40.6 m^3/s) (Figure 9c). The percent errors of the simulated peak flow values through the original SWAT model and the modified SWAT model compared to the observed peak flow values were 13.2% and 13.9%, respectively, showing no significant difference. However, the hourly flow prediction performance of the modified SWAT model was better than the original SWAT model, with an R^2 of 0.88, NSE of 0.84, and PBIAS of 23.9%, compared with an R^2 of 0.85, NSE of 0.75, and PBIAS of 38.5% for the original model. For event 6, both models underestimated the peak flow due to anthropogenic factors such as reservoir discharge and drainage from submerged paddy fields not reflected in the models (Figure 9f). In event 8 (precipitation 114.5 mm, peak flow 57.6 m^3/s), the peak flow of the original SWAT model and the modified SWAT model are 73.4 m^3/s and 54.5 m^3/s, respectively, and are simulated after a 2 h delay from the observation time (13 July 2022 22:00 h) of the peak flow (Figure 9h). The observed peak flow errors compared to the simulations by the original and modified SWAT models were 27.4% and 5.4%, respectively. This study has shown that the modified SWAT model can predict both long-term continuous time-series hourly flow and overall peak flow for rainfall events with excellent performance.

4. Discussion

The findings of this study demonstrate the improved performance of the modified SWAT model in predicting long-term continuous hourly flow and overall peak flow for rainfall events. Sensitive parameters for hourly flow simulation were consistently identified in both models, showing similarity to sensitivity ranking results from other hourly SWAT modeling studies [62,64,65]. But, there were significant differences between the models in the calibration values of some parameters.

Romanowicz et al. [66] suggest that the hydrological response of the SWAT model is highly sensitive to the quality of soil and land use data, as well as to the pre-processing procedures of geographically distributed data. This indicates that changes in the initial values of spatially distributed soil parameters and the soil moisture algorithm can have significant impacts on the sensitivity analysis process. The sensitivity analysis results can vary significantly based on methodological procedures, such as changes in input variables and the number of iterations, as well as the length of observation data [67]. In particular, the effect on parameters is proven to be higher in the hourly SWAT model simulation than in the daily SWAT model simulation [68]. Therefore, a substantial amount of observation data will be required to accurately determine the most sensitive parameter and to analyze parameter sensitivity using various methodological procedures.

We also found that the differences in soil moisture behavior by soil layer and spatial soil moisture distribution in the watershed simulated in the two models had a significant impact on hourly flow simulations during long-term and short-term rainfall events. Soil moisture plays an important role in determining surface runoff, infiltration, and the amount of water flowing into groundwater. Fuka et al. [69] have shown that adjusting soil properties based on topography can enable more accurate soil characterization and improve the flow prediction performance of the model. Moreover, the utilization of remote sensing soil moisture data has the potential to reduce calibration uncertainties and enhance flow predictions [70]. This shows that the reflection of spatial soil properties redistributed using remote sensing and physical soil moisture behavior characteristics within the SWAT model contributed to better hourly flow simulation than the original model. The findings of our study emphasize the importance of initialization considering the spatial distribution of soil parameters and soil moisture estimation based on physical processes in calibrating the hourly flow of the SWAT model.

Nevertheless, this study has several major limitations. The soil moisture in this study could not be verified due to the absence of observation data. The physical feasibility of the selected set of soil parameters can be assessed through validation against spatially distributed soil moisture observations. Additionally, temporally occurring cracks due to the drying process of the soil can lead to significant changes in the hydraulic properties of the soil [71]. This indicates the need for future studies to adjust soil parameters to reflect soil moisture conditions over time, as well as the spatial characteristics of soil parameters. These adjustments could play an important role in further understanding the interaction between the spatial distribution of soil moisture and climate change, and in more accurately predicting soil moisture and flow. Furthermore, this study relied on data from a single meteorological station for hourly flow simulations. In watershed-scale rainfall–runoff modeling, integrating spatial rainfall data is very important for enhancing the robustness of models in predicting initial soil moisture conditions and rainfall events [72]. To enhance the hourly peak flow prediction performance of the hourly SWAT model, future studies need to supplement it with spatial rainfall data. This will enable the model to capture the spatial variability of rainfall in the watershed and improve the accuracy of hourly flow simulations.

5. Conclusions

The SWAT model has gained popularity in simulating hourly flow in watersheds of various sizes and identifying areas at risk of floods. However, the model was originally designed for long-term simulations at a daily time scale and uses a semi-distributed structure. Therefore, it requires modifications to accurately simulate hourly flow and consider spatiotemporal soil moisture variability based on high-resolution rainfall data.

To address these limitations, this study linked a Noah LSM with a physical soil moisture process based on the Richards equation to the SWAT model. Furthermore, the hydrological soil parameters within the watershed were spatially distributed using surface soil moisture based on remote sensing soil moisture images. The modified SWAT model was then applied to a 52 km^2 agricultural watershed, and its hourly flow prediction performance was analyzed and compared to the original SWAT model.

We found that the spatial distribution approach of hydrological soil parameters based on remote sensing soil moisture images contributed to improving the spatial distribution problem of soil moisture in the watershed without the assimilation of any field soil moisture observation data. Our findings suggest that improvements in soil moisture routing and soil parameter distribution in the SWAT model could reduce hourly flow prediction errors for multiple rainfall events and long-term continuous periods. Although the modified SWAT model integrated showed improvements in hourly flow prediction performance, it is important to consider the influence of anthropogenic activities in the watershed in the hydrological modeling process to increase the efficiency of multilateral interpretations of the hydrologic simulation results. Furthermore, calibration with spatially distributed hydrological observation data and in situ soil moisture measurements can be explored as potential methods to reduce model parameter uncertainty and verify the physical feasibility of the soil parameter set. The modified SWAT model is a stand-alone engine, internally designed to calculate hourly soil moisture and flow with a physical soil moisture module. This allows for a flexible application in watersheds with diverse soil, vegetation, and climate conditions. The methodology for redistributing soil parameter properties using remotely sensed soil moisture data can be applied to suit the soil characteristics of different watersheds. This suggests that the modified SWAT model has the potential to sufficiently extend hourly flow predictions to a variety of watersheds. Although this study was conducted in a specific agricultural watershed, further validation through application to a diverse range of watersheds is necessary.

The methodology of this study can be used in a modeling approach for integrated simulation of soil moisture and hourly flow based on physical processes at the watershed scale. Furthermore, it is expected to provide the scientific community, water management, and agricultural experts with in-depth information for dam operations, disaster prevention, and crop yield improvement.

Author Contributions: Conceptualization, S.L. and J.K.; methodology, S.L. and K.J.L.; formal analysis, S.L.; data curation, S.L.; writing—original draft preparation, S.L.; writing—review and editing, J.K. and K.J.L.; visualization, S.L.; supervision, J.K. All authors have read and agreed to the published version of the manuscript.

Funding: This study was supported by "Korea Environment Industry & Technology Institute (KEITI) through the Aquatic Ecosystem Conservation Research Program, funded by the Korea Ministry of Environment (MOE), grant number 2020003030004" and "2021 Research Grant from Kangwon National University".

Institutional Review Board Statement: Not applicable.

Informed Consent Statement: Not applicable.

Data Availability Statement: The data that support the findings of this study are available from the corresponding author upon reasonable request.

Conflicts of Interest: The authors declare no conflicts of interest.

References

1. Modi, P.A.; Czuba, J.A.; Easton, Z.M. Coupling a Land Surface Model with a Hydrodynamic Model for Regional Flood Risk Assessment Due to Climate Change: Application to the Susquehanna River near Harrisburg, Pennsylvania. *J. Flood Risk Manag.* **2022**, *15*, e12763. [CrossRef]
2. Huang, H.; Cui, H.; Ge, Q. Assessment of Potential Risks Induced by Increasing Extreme Precipitation under Climate Change. *Nat. Hazards* **2021**, *108*, 2059–2079. [CrossRef]
3. Diakakis, M.; Deligiannakis, G.; Antoniadis, Z.; Melaki, M.; Katsetsiadou, N.K.; Andreadakis, E.; Spyrou, N.I.; Gogou, M. Proposal of a Flash Flood Impact Severity Scale for the Classification and Mapping of Flash Flood Impacts. *J. Hydrol.* **2020**, *590*, 125452. [CrossRef]
4. Ching, Y.C.; Lee, Y.H.; Toriman, M.E.; Abdullah, M.; Yatim, B. Bin Effect of the Big Flood Events on the Water Quality of the Muar River, Malaysia. *Sustain. Water Resour. Manag.* **2015**, *1*, 97–110. [CrossRef]
5. Janizadeh, S.; Chandra Pal, S.; Saha, A.; Chowdhuri, I.; Ahmadi, K.; Mirzaei, S.; Mosavi, A.H.; Tiefenbacher, J.P. Mapping the Spatial and Temporal Variability of Flood Hazard Affected by Climate and Land-Use Changes in the Future. *J. Environ. Manag.* **2021**, *298*, 113551. [CrossRef]
6. Arnold, J.G.; Srinivasan, R.; Muttiah, R.S.; Williams, J.R. Large Area Hydrologic Modelling and Assessment. Part I—Model Development. *J. Am. Water Resour. Assoc.* **1998**, *34*, 73–89. [CrossRef]
7. Bicknell, B.R.; Imhoff, J.C.; Kittle, J.L., Jr.; Donigan, A.S., Jr.; Johanson, R.C.; Barnwell, T.O. *Hydrological Simulation Program—Fortran User's Manual for Release 11*; U.S. Environmental Protection Agency: Athens, GA, USA, 1996; p. 100.
8. Tan, M.L.; Gassman, P.W.; Raghavan, S.; Arnold, J.G.; Yang, X. A Review of SWAT Studies in Southeast Asia: Applications, Challenges and Future Directions. *Water* **2019**, *11*, 914. [CrossRef]
9. Van Griensven, A.; Ndomba, P.; Yalew, S.; Kilonzo, F. Critical Review of SWAT Applications in the Upper Nile Basin Countries. *Hydrol. Earth Syst. Sci.* **2012**, *16*, 3371–3381. [CrossRef]
10. Akoko, G.; Le, T.H.; Gomi, T.; Kato, T. A Review of SWAT Model Application in Africa. *Water* **2021**, *13*, 1313. [CrossRef]
11. Aloui, S.; Mazzoni, A.; Elomri, A.; Aouissi, J.; Boufekane, A.; Zghibi, A. A Review of Soil and Water Assessment Tool (SWAT) Studies of Mediterranean Catchments: Applications, Feasibility, and Future Directions. *J. Environ. Manag.* **2023**, *326*, 116799. [CrossRef] [PubMed]

12. Jeong, J.; Kannan, N.; Arnold, J.; Glick, R.; Gosselink, L.; Srinivasan, R. Development and Integration of Sub-Hourly Rainfall-Runoff Modeling Capability Within a Watershed Model. *Water Resour. Manag.* **2010**, *24*, 4505–4527. [CrossRef]
13. Yu, D.; Xie, P.; Dong, X.; Hu, X.; Liu, J.; Li, Y.; Peng, T.; Ma, H.; Wang, K.; Xu, S. Improvement of the SWAT model for event-based flood simulation on a sub-daily timescale. *Hydrol. Earth Syst. Sci.* **2018**, *22*, 5001–5019. [CrossRef]
14. Li, Y.; DeLiberty, T. Evaluating Hourly SWAT Streamflow Simulations for Urbanized and Forest Watersheds across Northwestern Delaware, US. *Stoch. Environ. Res. Risk Assess.* **2021**, *35*, 1145–1159. [CrossRef]
15. Qi, J.; Zhang, X.; McCarty, G.W.; Sadeghi, A.M.; Cosh, M.H.; Zeng, X.; Gao, F.; Daughtry, C.S.T.; Huang, C.; Lang, M.W.; et al. Assessing the Performance of a Physically-Based Soil Moisture Module Integrated within the Soil and Water Assessment Tool. *Environ. Model. Softw.* **2018**, *109*, 329–341. [CrossRef]
16. de Andrade, C.W.L.; Montenegro, S.M.G.L.; Montenegro, A.A.A.; Lima, J.R.d.S.; Srinivasan, R.; Jones, C.A. Soil Moisture and Discharge Modeling in a Representative Watershed in Northeastern Brazil Using SWAT. *Ecohydrol. Hydrobiol.* **2019**, *19*, 238–251. [CrossRef]
17. Shin, S.; Park, G.; Lee, S.; Shin, Y.; Jang, K.; Chun, J.; Kim, J. Soil Parameter Estimation Technology Based on Hydrological Connectivity to Predict Spatially Distributed Soil Moisture. *J. Agric. Life Environ. Sci.* **2022**, *34*, 287–300. [CrossRef]
18. Al-Shrafany, D.; Rico-Ramirez, M.A.; Han, D.; Bray, M. Comparative Assessment of Soil Moisture Estimation from Land Surface Model and Satellite Remote Sensing Based on Catchment Water Balance. *Meteorol. Appl.* **2014**, *21*, 521–534. [CrossRef]
19. Ho-Hagemann, H.T.M.; Hagemann, S.; Rockel, B. On the Role of Soil Moisture in the Generation of Heavy Rainfall during the Oder Flood Event in July 1997. *Tellus A Dyn. Meteorol. Oceanogr.* **2015**, *67*, 28661. [CrossRef]
20. Blume, T.; Zehe, E.; Bronstert, A. Use Soil Moisture Dynamics and Patterns at Different Spatio-Temporal Scales for the Investigation of Subsurface Flow Processes. *Hydrol. Earth Syst. Sci.* **2009**, *13*, 1215–1233. [CrossRef]
21. Maxwell, R.M.; Lundquist, J.K.; Mirocha, J.D.; Smith, S.G.; Woodward, C.S.; Tompson, A.F.B. Development of a Coupled Groundwater–Atmosphere Model. *Mon. Weather Rev.* **2011**, *139*, 96–116. [CrossRef]
22. Wagner, S.; Fersch, B.; Yuan, F.; Yu, Z.; Kunstmann, H. Fully Coupled Atmospheric-Hydrological Modeling at Regional and Long-Term Scales: Development, Application, and Analysis of WRF-HMS. *Water Resour. Res.* **2016**, *52*, 3187–3211. [CrossRef]
23. Yuan, F.; Kunstmann, H.; Yang, C.; Yu, Z.; Ren, L.; Fersch, B.; Xie, Z. *Development of a Coupled Land-Surface and Hydrology Model System for Mesoscale Hydrometeorological Simulations*; IAHS Publication: Wallingford, UK, 2009; Volume 333, pp. 195–202.
24. Livneh; Restrepo, P.J.; Lettenmaier, D.P. Development of a Unified Land Model for Prediction of Surface Hydrology and Land-Atmosphere Interactions. *J. Hydrometeor.* **2011**, *12*, 1299–1320. [CrossRef]
25. Zhuo, L.; Dai, Q.; Han, D.; Chen, N.; Zhao, B. Assessment of Simulated Soil Moisture from WRF Noah, Noah-MP, and CLM Land Surface Schemes for Landslide Hazard Application. *Hydrol. Earth Syst. Sci.* **2019**, *23*, 4199–4218. [CrossRef]
26. Alvarez-Garreton, C.; Ryu, D.; Western, A.W.; Su, C.H.; Crow, W.T.; Robertson, D.E.; Leahy, C. Improving Operational Flood Ensemble Prediction by the Assimilation of Satellite Soil Moisture: Comparison between Lumped and Semi-Distributed Schemes. *Hydrol. Earth Syst. Sci.* **2015**, *19*, 1659–1676. [CrossRef]
27. Williams, J.R. Flood Routing with Variable Travel Time or Variable Storage Coefficients. *Trans. ASABE* **1969**, *12*, 100–103. [CrossRef]
28. Overton, D.E. Muskingum Flood Routing of Upland Streamflow. *J. Hydrol.* **1966**, *4*, 185–200. [CrossRef]
29. Neitsch, S.; Arnold, J.; Kinry, J.R.; Williams, J.R. Soil and Water Assessment Tool Theoretical Documentation Version 2009. Texas Water Resources Institute. Available online: https://swat.tamu.edu/docs/ (accessed on 8 February 2024).
30. Mein, R.G.; Larson, C.L. Modeling Infiltration during a Steady Rain. *Water Resour. Res.* **1973**, *9*, 384–394. [CrossRef]
31. Nearing, M.A.; Liu, B.Y.; Risse, L.M.; Zhang, X. Curve Numbers and Green-Ampt Effective Hydraulic Conductivities1. *JAWRA J. Am. Water Resour. Assoc.* **1996**, *32*, 125–136. [CrossRef]
32. Ek, M.; Mitchell, K.; Lin, Y.; Rogers, E.; Grunmann, P.; Koren, V.; Gayno, G.; Tarpley, J. Implementation of NOAH Land Surface Model Advances in the National Centers for Environmental Prediction Operational Mesoscale Eta Model. *J. Geophys. Res.* **2003**, *108*, 8851. [CrossRef]
33. Richards, L.A. Capillary Conduction of Liquids Through Porous Mediums. *Physics* **1931**, *1*, 318–333. [CrossRef]
34. Sahoo, A.K.; Dirmeyer, P.A.; Houser, P.R.; Kafatos, M. A Study of Land Surface Processes Using Land Surface Models over the Little River Experimental Watershed, Georgia. *J. Geophys. Res. Atmos.* **2008**, *113*. [CrossRef]
35. Eweys, O.A.; Elwan, A.A.; Borham, T.I. Integrating WOFOST and Noah LSM for Modeling Maize Production and Soil Moisture with Sensitivity Analysis, in the East of The Netherlands. *Field Crops Res.* **2017**, *210*, 147–161. [CrossRef]
36. Clapp, R.B.; Hornberger, G.M. Empirical Equations for Some Soil Hydraulic Properties. *Water Resour. Res.* **1978**, *14*, 601–604. [CrossRef]
37. Niu, G.-Y.; Yang, Z.-L.; Mitchell, K.E.; Chen, F.; Ek, M.B.; Barlage, M.; Kumar, A.; Manning, K.; Niyogi, D.; Rosero, E.; et al. The Community Noah Land Surface Model with Multiparameterization Options (Noah-MP): 1. Model Description and Evaluation with Local-Scale Measurements. *J. Geophys. Res. Atmos.* **2011**, *116*. [CrossRef]
38. Zeyliger, A.M.; Muzalevskiy, K.V.; Zinchenko, E.V.; Ermolaeva, O.S. Field Test of the Surface Soil Moisture Mapping Using Sentinel-1 Radar Data. *Sci. Total Environ.* **2022**, *807*, 151121. [CrossRef]
39. Zhang, X.; Chan, N.W.; Pan, B.; Ge, X.; Yang, H. Mapping Flood by the Object-Based Method Using Backscattering Coefficient and Interference Coherence of Sentinel-1 Time Series. *Sci. Total Environ.* **2021**, *794*, 148388. [CrossRef]

40. Benzougagh, B.; Frison, P.-L.; Meshram, S.G.; Boudad, L.; Dridri, A.; Sadkaoui, D.; Mimich, K.; Khedher, K.M. Flood Mapping Using Multi-Temporal Sentinel-1 SAR Images: A Case Study—Inaouene Watershed from Northeast of Morocco. *Iran. J. Sci. Technol. Trans. Civ. Eng.* **2022**, *46*, 1481–1490. [CrossRef]
41. Kim, S.; Lee, T.; Shin, Y. Estimation of High-Resolution Soil Moisture Based on Sentinel-1A/B SAR Sensors. *J. Korean Soc. Agric. Eng.* **2019**, *61*, 89–99. [CrossRef]
42. Şekertekin, A.; Marangoz, A.M.; Abdikan, S. Soil Moisture Mapping Using Sentinel-1A Synthetic Aperture Radar Data. *Int. J. Environ. Geoinform.* **2018**, *5*, 178–188. [CrossRef]
43. Lee, S.; Hong, S.; Cho, J.; Lee, Y. Experimental Retrieval of Soil Moisture for Cropland in South Korea Using Sentinel-1 SAR Data. *Korean J. Remote Sens.* **2017**, *33*, 947–960. [CrossRef]
44. Khaldoune, J.; van Bochove, E.; Bernier, M.; Nolin, M. Mapping Agricultural Frozen Soil on the Watershed Scale Using Remote Sensing Data. *Appl. Environ. Soil Sci.* **2011**, *2011*, 193237. [CrossRef]
45. Kannan, N.; White, S.M.; Worrall, F.; Whelan, M.J. Sensitivity Analysis and Identification of the Best Evapotranspiration and Runoff Options for Hydrological Modelling in SWAT-2000. *J. Hydrol.* **2007**, *332*, 456–466. [CrossRef]
46. Abbaspour, K.C.; Vejdani, M.; Haghighat, S.; Yang, J. SWAT-CUP Calibration and Uncertainty Programs for SWAT. In Proceedings of the MODSIM 2007 International Congress on Modelling and Simulation, Society of Australia and New Zealand, Dübendorf, Switzerland, 10–13 December 2007; pp. 1596–1602.
47. Alodah, A.; Seidou, O. The Adequacy of Stochastically Generated Climate Time Series for Water Resources Systems Risk and Performance Assessment. *Stoch. Environ. Res. Risk Assess.* **2019**, *33*, 253–269. [CrossRef]
48. Araza, A.; Perez, M.; Cruz, R.V.; Aggabao, L.F.; Soyosa, E. Probable Streamflow Changes and Its Associated Risk to the Water Resources of Abuan Watershed, Philippines Caused by Climate Change and Land Use Changes. *Stoch. Environ. Res. Risk Assess.* **2021**, *35*, 389–404. [CrossRef]
49. Khatun, S.; Sahana, M.; Jain, S.K.; Jain, N. Simulation of Surface Runoff Using Semi Distributed Hydrological Model for a Part of Satluj Basin: Parameterization and Global Sensitivity Analysis Using SWAT CUP. *Model. Earth Syst. Environ.* **2018**, *4*, 1111–1124. [CrossRef]
50. Mengistu, A.G.; van Rensburg, L.D.; Woyessa, Y.E. Techniques for Calibration and Validation of SWAT Model in Data Scarce Arid and Semi-Arid Catchments in South Africa. *J. Hydrol. Reg. Stud.* **2019**, *25*, 100621. [CrossRef]
51. Singh, V.; Bankar, N.; Salunkhe, S.S.; Bera, A.K.; Sharma, J.R. Hydrological Stream Flow Modelling on Tungabhadra Catchment: Parameterization and Uncertainty Analysis Using SWAT CUP. *Curr. Sci.* **2013**, *104*, 1187–1199.
52. Rouholahnejad, E.; Abbaspour, K.C.; Vejdani, M.; Srinivasan, R.; Schulin, R.; Lehmann, A. A Parallelization Framework for Calibration of Hydrological Models. *Environ. Model. Softw.* **2012**, *31*, 28–36. [CrossRef]
53. Wu, H.; Chen, B. Evaluating Uncertainty Estimates in Distributed Hydrological Modeling for the Wenjing River Watershed in China by GLUE, SUFI-2, and ParaSol Methods. *Ecol. Eng.* **2015**, *76*, 110–121. [CrossRef]
54. Maharjan, G.R.; Park, Y.S.; Kim, N.W.; Shin, D.S.; Choi, J.W.; Hyun, G.W.; Jeon, J.-H.; Ok, Y.S.; Lim, K.J. Evaluation of SWAT Sub-Daily Runoff Estimation at Small Agricultural Watershed in Korea. *Front. Environ. Sci. Eng.* **2013**, *7*, 109–119. [CrossRef]
55. Abbaspour, K.C.; Vaghefi, S.A.; Srinivasan, R. A Guideline for Successful Calibration and Uncertainty Analysis for Soil and Water Assessment: A Review of Papers from the 2016 International SWAT Conference. *Water* **2017**, *10*, 6. [CrossRef]
56. Moriasi, D.; Arnold, J.G.; Van Liew, M.W.; Bingner, R.L.; Harmel, R.D.; Veith, T.L. Model Evaluation Guidelines for Systematic Quantification of Accuracy in Watershed Simulations. *Trans. ASABE* **2007**, *50*, 885–900. [CrossRef]
57. Nash, J.E.; Sutcliffe, J.V. River Flow Forecasting through Conceptual Models Part I—A Discussion of Principles. *J. Hydrol.* **1970**, *10*, 282–290. [CrossRef]
58. Gupta, H.V.; Sorooshian, S.; Yapo, P.O. Status of Automatic Calibration for Hydrologic Models: Comparison with Multilevel Expert Calibration. *J. Hydrol. Eng.* **1999**, *4*, 135–143. [CrossRef]
59. Moriasi, D.; Gitau, M.; Pai, N.; Daggupati, P. Hydrologic and Water Quality Models: Performance Measures and Evaluation Criteria. *Trans. ASABE Am. Soc. Agric. Biol. Eng.* **2015**, *58*, 1763–1785. [CrossRef]
60. Neitsch, S.L.; Arnold, J.G.; Kiniry, J.R.; Srinivasan, R.; Williams, J.R. *Soil and Water Assessment Tool: User's Manual Version 2000*; TWRI Report TR-192; Texas Water Resource Institute: College Station, TX, USA, 2002.
61. Tejaswini, V.; Sathian, K.K. Calibration and Validation of Swat Model for Kunthipuzha Basin Using SUFI-2 Algorithm. *Int. J. Curr. Microbiol. Appl. Sci.* **2018**, *7*, 2162–2172. [CrossRef]
62. Boithias, L.; Sauvage, S.; Lenica, A.; Roux, H.; Abbaspour, K.C.; Larnier, K.; Dartus, D.; Sánchez-Pérez, J.M. Simulating Flash Floods at Hourly Time-Step Using the SWAT Model. *Water* **2017**, *9*, 929. [CrossRef]
63. Shannak, S.D. Calibration and Validation of Swat for Sub-Hourly Time Steps Using Swat- Calibration and Validation Of Swat For Sub-Hourly Time Steps Using Swat-Cup. *Int. J. Sustain. Water Environ. Syst.* **2017**, *9*, 21–27.
64. Li, D.; Qu, S.; Shi, P.; Chen, X.; Xue, F.; Gou, J.; Zhang, W. Development and Integration of Sub-Daily Flood Modelling Capability within the SWAT Model and a Comparison with XAJ Model. *Water* **2018**, *10*, 1263. [CrossRef]
65. Koltsida, E.; Mamassis, N.; Kallioras, A. Hydrological Modeling Using the SWAT Model in Urban and Peri-Urban Environments: The Case of Kifissos Experimental Sub-Basin (Athens, Greece). *Hydrol. Earth Syst. Sci.* **2023**, *27*, 917–931. [CrossRef]
66. Romanowicz, A.A.; Vanclooster, M.; Rounsevell, M.; La Junesse, I. Sensitivity of the SWAT Model to the Soil and Land Use Data Parametrisation: A Case Study in the Thyle Catchment, Belgium. *Ecol. Modell.* **2005**, *187*, 27–39. [CrossRef]

67. Moreira, L.; Schwamback, D.; Rigo, D. Sensitivity Analysis of the Soil and Water Assessment Tools (SWAT) Model in Streamflow Modeling in a Rural River Basin. *Ambient. Agua Interdiscip. J. Appl. Sci.* **2018**, *13*, 1. [CrossRef]
68. Yang, X.; Liu, Q.; He, Y.; Luo, X.; Zhang, X. Comparison of Daily and Sub-Daily SWAT Models for Daily Streamflow Simulation in the Upper Huai River Basin of China. *Stoch. Environ. Res. Risk Assess.* **2016**, *30*, 959–972. [CrossRef]
69. Fuka, D.R.; Collick, A.S.; Kleinman, P.J.A.; Auerbach, D.A.; Harmel, R.D.; Easton, Z.M. Improving the Spatial Representation of Soil Properties and Hydrology Using Topographically Derived Initialization Processes in the SWAT Model. *Hydrol. Process.* **2016**, *30*, 4633–4643. [CrossRef]
70. Kundu, D.; Vervoort, R.W.; van Ogtrop, F.F. The Value of Remotely Sensed Surface Soil Moisture for Model Calibration Using SWAT. *Hydrol. Process.* **2017**, *31*, 2764–2780. [CrossRef]
71. An, R.; Wang, Y.; Zhang, X.; Chen, C.; Liu, X.; Cai, S. Quantitative Characterization of Drying-Induced Cracks and Permeability of Granite Residual Soil Using Micron-Sized X-ray Computed Tomography. *Sci. Total Environ.* **2023**, *876*, 163213. [CrossRef]
72. Tramblay, Y.; Bouvier, C.; Ayral, P.-A.; Marchandise, A. Impact of Rainfall Spatial Distribution on Rainfall-Runoff Modelling Efficiency and Initial Soil Moisture Conditions Estimation. *Nat. Hazards Earth Syst. Sci.* **2011**, *11*, 157–170. [CrossRef]